First Middle East Conference on Smart Monitoring,
Assessment and Rehabilitation of Civil Structures
8 – 10 February 2011, Dubai, UAE

SMAR 2011

Slenderness ratio effect on the behavior of steel and carbon-FRP reinforced concrete-filled FRP tubes

H. M. Mohamed[1], R. Masmoudi[2], and Y. Shao[3]

[1] Postdoctoral Fellow, University of Sherbrooke, Sherbrooke, QC, Canada
[2] Professor, University of Sherbrooke, Sherbrooke, QC, Canada
[3] Professor, McGill University, Montreal, QC, Canada

ABSTRACT: Concrete-filled fiber-reinforced polymer (FRP) tubes (CFFTs) system is one of the most promising techniques to protect the reinforced concrete structures from aggressive environmental conditions. This paper presents the results of an experimental investigation on the strength and failure modes of ten CFFT columns. The effect of two parameters and their interactions on the buckling behavior were investigated; namely, the type of internal reinforcement (steel or carbon FRP bars) and the slenderness ratio. The eleven CFFT columns of different slenderness ratio 4, 8, 12, 16 and 20 were tested under pure compression load. The internal diameter and the thickness of the FRP tubes are 152 mm and 2.65 mm, respectively. The test results indicated that the axial compressive strength of steel and CFRP-reinforced CFFT columns was reduced by 13% to 32% with increasing the slenderness ratio from 4 to 20. Also, it was found that the axial capacity of CFRP-reinforced CFFT columns resulted in average 12.5% reduction as compared to the counterpart steel-reinforced CFFT columns.

1 INTRODUCTION

The application of composite materials has been propagated by the deterioration of the old conventional concrete, steel, and timber structures (Masmoudi et al. 1998). The fiber-reinforced polymers (FRP) tubes can play an important role in replacing transverse steel by providing ductility and strength for reinforced concrete columns (Mohamed and Masmoudi 2008 and 2010; Mirmiran et al. 2001). The use of FRP composite tubes in civil engineering applications offers several advantages such as confinement, protecting the concrete core, providing shear or/and flexural reinforcement and finally, act as a permanent formwork which save the time and cost of the construction. In recent years, some applications of concrete-filled FRP tubes (CFFTs) technique for different structural applications piles, columns, girders, bridge piers were accomplished (Fam et al. 2003). FRP bars are well known for their high tensile mechanical properties and are being used more and more in lieu of steel reinforcements, because of their resistance to corrosion and their long term durability. Until now, the FRP-design guidelines and codes worldwide have not recommended the use of FRP bars in compression. This is attributed to the fact that very few studies have been conducted on FRP bars as compression reinforcements. This has made it necessary to create a comprehensive study to insure their safe application for different concrete structures. Combining the advantages of FRP bars with CFFT technique will lead to a fully noncorrosive structure. Research studies conducted to evaluate the behavior of the FRP bars under compression loads are very limited. Compressive capacity of FRP bars has been investigated by Wu (1999). It was reported that the compressive strength of

First Middle East Conference on Smart Monitoring,
Assessment and Rehabilitation of Civil Structures
8 – 10 February 2011, Dubai, UAE

SMAR 2011

glass and carbon FRP bars were 55% and 78%, respectively, of their tensile strength. Similar study was conducted by Kobayashi and Fujisaki (1995). It was found that the compressive capacity of glass and carbon FRP bars were 30% and 30 to 50% of their tensile strength, respectively. An experimental program has been conducted by Alsayed et al. (2000) to investigate the behavior of glass FRP-reinforced concrete (RC) columns versus convention steel-RC columns. It was found that the glass FRP-RC columns resulted in approximately 10% reduction in concentric capacity as compared to steel-RC columns. Choo et al. (2006) investigated the strength of rectangular RC columns reinforced with FRP bars. It was reported that ignoring the contribution of the FRP reinforcements in the compression zone might be conservative. On the other hand, several researchers had studied many parameters for the FRP closed forms, particularly CFFT. Mohamed et al. (2010) conducted analytical nonlinear stability analysis beside an experimental investigation on the behavior of CFFT columns. The test results indicated that increasing the slenderness ratio from 8 to 20, decreased the load carrying capacities of the CFFT specimens by 30%. Also, the analytical study indicated that the inelastic tangent Euler buckling load could be used to control the instability load of CFFT columns. It gives very conservative prediction for the reinforced CFFT columns under axial loads.

This paper presents an experimental investigation on the buckling responses of CFFT columns. The experimental program included testing of eleven CFFT columns with various slenderness ratios. The main objective of this paper is to evaluate the performance of CFRP-rebar against the steel-rebar as compression reinforcement for short and long heights CFFT columns.

2   EXPERIMENTAL PROGRAM

2.1   *Materials Properties*

2.1.1   GFRP tubes

FRP tubes with an internal diameter of 152 mm were used in the experimental program. The FRP tubes were fabricated using filament winding technique; E-glass fiber and Epoxy resin were utilized for manufacturing these tubes. The split-disk and coupon tensile tests were performed on five specimens according to the ASTM D-2290-08 and ASTM D 638-08 standard. Table 1 shows the details, dimensions and the mechanical properties the used FRP tubes.

Table 1. Dimension and mechanical properties of FRP tubes

| Diameter (mm) | Thickness (mm) | Stacking sequence | Hoop | | | Axial | | |
			Young's modulus (MPa)	Ultimate strength (MPa)	Ultimate strain (%)	Young's modulus (MPa)	Ultimate strength (MPa)	Ultimate strain (%)
152	2.65	$[\pm 60]_3$	10385	348	3.88	12808	60.10	0.932

2.1.2   Concrete

All specimens in this study were constructed from one type of normal concrete strength. Concrete batch was supplied by ready mix concrete supplier. Five plain concrete cylinders (152x305 mm) were prepared and cured under the same conditions as the test specimens. The 28-day average concrete compressive strength was found equal to 30 ±0.6 MPa.

2.1.3   Carbon FRP bars

Sand-coated carbon FRP (CFRP) bars No. 3 were used as longitudinal reinforcement for the columns. The CFRP bars were manufactured and developed by Pultrall Inc., Quebec, Canada.

First Middle East Conference on Smart Monitoring,
Assessment and Rehabilitation of Civil Structures
8 – 10 February 2011, Dubai, UAE

SMAR 2011

The bars were made of continuous fiber impregnated in vinylester resin with a fiber content of 73%, using the pultrusion process. Table 2 presents the mechanical properties of the CFRP bars.

Table 2 — Properties of reinforcing CFRP bars

US size	Nominal diameter (mm)	Nominal area (mm²)	Tensile modulus of elasticity (GPa)	Ultimate tensile strength (MPa)	Ultimate strain (%)
#3	9.52	71.26	128±5	1431	1.20±0.09

2.1.4 Steel bars

Deformed steel bars No.10M were used as a longitudinal reinforcement for the steel-reinforced CFFT columns. The mechanical properties of the steel bars were obtained from standard tests that were carried out according to ASTM A615/A615M-09, on five specimens. The average values of the yield and ultimate tensile strength were 462 and 577 MPa, respectively.

2.2 Test Specimens

The objective of the experimental program is to investigate the slenderness effects on the behavior of CFFT columns under pure compression loads. The test specimens are classified for three groups. Table 3 summarizes the different configurations and details of the test specimens. The main parameters investigated include the type of internal reinforcements and the slenderness ratio of the columns. In this paper, the slenderness ratio kl/r was calculated based on the geometric characteristics of the concrete neglecting the contribution of the FRP tubes (k and l are, respectively, the column effective length factor and height). The radius of gyration r is computed as $\sqrt{I/A_g}$, where I and A_g are the moment of inertia and the gross section of the column respectively. This assumption was based on the small thickness of the FRP tubes besides the fact that the fiber orientations of the tubes were oriented mainly toward the hoop direction rather than the axial direction. Another assumption was taken throughout the manuscript that was the tested specimens represent the case of fixed-fixed columns with (k =0.5). The test specimens were identified by codes listed in the second column of Table 3. The first number presents the slenderness ratio of the specimens. The identifications W, S and C were used to present the type of internal reinforcements, without internal reinforcements, steel bars and CFRP bars, respectively. The second number shows the height of the specimen in (cm), whereas, the height is ranged between 305 mm to 1520 mm. Group No. 1 presents three CFFT cylinders proposed in the test matrix to obtain the ultimate confined concrete compressive strength. Group No. 2 and 3 present CFFT columns reinforced internally with steel bars (6 No. 10M) and CFRP bars (6 No. 3), respectively, with slenderness ratio varied from 8 to 20. The bars were distributed uniformly inside the cross section of the GFRP tube. A concrete cover of 10 mm was provided between the ends of the longitudinal steel bars and the top and bottom surfaces of the specimens to avoid the stress concentration at the steel bars area. Figure 1 shows the steel and CFRP cages for the CFFT columns.

First Middle East Conference on Smart Monitoring,
Assessment and Rehabilitation of Civil Structures
8 – 10 February 2011, Dubai, UAE

SMAR 2011
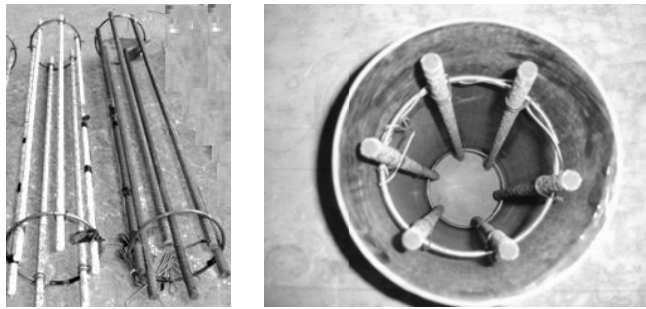
CFRP cage   Steel cage   Overview for cage and tube inside the wooden formwork

Figure 1. Typical cages from steel and CFRP bars for RCFFT columns

Table 3. Specimens details and summary of test results

Group No.	ID	l (mm)	kl/r	Internal reinforcement		P_y (kN)	P_u (kN)	f'_{cc} (MPa)	f'_{cc}/f'_c
1	4-W-30[a]	305	4	----		--	1316	74.2	2.47
2	8-S-60	610	8	Steel bars	6 - 10M	890	1652	78.4	2.61
	12-S-90	912	12			935	1454	67.1	2.24
	16-S-120	1216	16			996	1202	52.7	1.76
	20-S-150	1520	20			1086	1127	46.5	1.55
3	8-C-60	610	8	CFRP bars	6 - #3	--	1432	67.04	2.23
	12-C-90	912	12			--	1343	62.02	2.07
	16-C-120	1216	16			--	1138	50.44	1.68
	20-C-150	1520	20			--	1127	49.82	1.66

a: average for three specimens

2.3 Instrumentation and Test Setup

Internal and external instrumentations were used in this study to capture the local strain distributions of the CFFT specimens. Before casting, two of the longitudinal steel or CFRP bars, 180 degree apart, were installed with the strain gauges at the mid height. Before testing, two axial and two hoop electrical resistance strain gauges were mounted, 180 degree apart, along the hoop direction on the external surface of the specimens. Strain gauges of 6 mm length were used to obtain the strain distribution from the steel and CFRP bars and the GFRP tubes surface. Strain gauges 30 mm were bonded on the surface of the concrete cylinders and control specimen reinforced with spiral steel bars. The axial displacement for each column was measured by two linear variable displacement transducers (LVDTs) 180 degrees apart along the hoop direction of the specimen. The LVDTs used have a maximum range of (100mm) with an accuracy of 0.01mm. Moreover, to measure the horizontal displacement, four LVDTs were mounted horizontally at the mid-height of the column 90 degrees around the column. All specimens were prepared before the test by a thin layer of high strength sulfur capping on the top and bottom surfaces to insure the uniform stress distribution during the test. The specimens were tested using a 6,000 kN capacity FORNEY machine, where the CFFT columns were setup vertically at the center of loading plates of the machine. The loading rate range was 2.0 to 2.50 kN/s during the test by manually controlling the loading rate of the hydraulic pump. Figure 2 shows the schematic of test setup and instrumentations used in this study.

First Middle East Conference on Smart Monitoring,
Assessment and Rehabilitation of Civil Structures
8 – 10 February 2011, Dubai, UAE

SMAR 2011
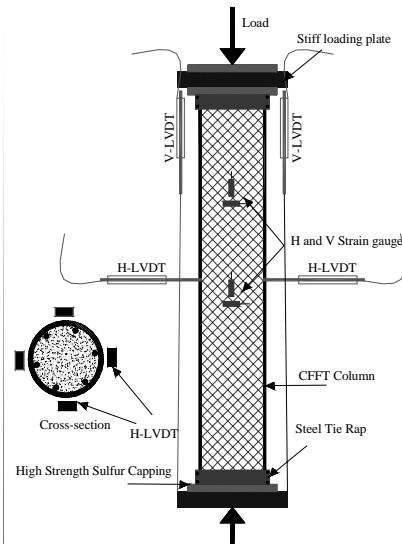
Figure 2. Schematic of test setup and instrumentations

3   RESULTS AND DISCUSSION

3.1   *Strength and Slenderness Ratio Effect*

The experimental yielding and ultimate loads, (P_y and P_u respectively) of all tested specimens are given in Table 3. In this Table, the confined concrete compressive strength f'_{cc} ; i.e., the maximum compressive strength just before failure and the effectiveness of the confining technique, f'_{cc}/f'_c are presented. The confined strength values for CFFT specimens without and with internal reinforcement were calculated using Equation 1, where A_g and A_{bars} are the column cross-section (internal area of FRP tubes) and the area of reinforcing bars (steel or CFRP), respectively. The compressive strength of the CFRP bars was considered to be equal a percentage ($\alpha = 40\%$) of the ultimate tensile strength (f_u), as suggested by Kobayashi and Fujisaki 1995.

$$f'_{cc} = \begin{cases} \dfrac{p_u}{A_g} & \text{Without internal reinforcement} \\[3mm] \dfrac{p_u - f_y A_{bars}}{A_g - A_{bars}} & \text{With steel bars} \\[3mm] \dfrac{p_u - \alpha f_u A_{bars}}{A_g - A_{bars}} & \text{With CFRP bars} \end{cases} \qquad (1)$$

The ultimate capacity of all specimens was depicted versus the slenderness ratio in Figure 10. Table 3 shows the increase in the axial strength of all specimens in terms of the ratio f'_{cc}/f'_c. Specimens in Group No.1 represented the case of short columns without internal longitudinal reinforcement (concrete cylinders). Although the modes of failure of the specimens in this group were similar to that of the specimens with slenderness ratio of 8 (rupture in the FRP tubes) their ultimate capacities were around 20% less than that of the specimens with ($kl/r = 8$). The difference in the ultimate capacities between the specimens that have different slenderness ratios

First Middle East Conference on Smart Monitoring,
Assessment and Rehabilitation of Civil Structures
8 – 10 February 2011, Dubai, UAE

SMAR 2011

resulted from the contribution of the internal reinforcement bars (neglecting the size effect). Theoretically speaking, considering the contribution of the internal reinforcement in calculating the ultimate capacity of the specimens in Group 1 ($f_y A_{bars}$) makes their failure loads similar to that of the specimens with ($kl/r =8$) (horizontal line at the beginning of the curves in Figure 3).

For all specimens, using FRP tubes to confine concrete columns increased the axial load carrying capacities regardless the slenderness ratio of the CFFT columns. Figure 10 confirms the fact that the ultimate load capacities of the CFFT specimens significantly decreased with increasing the slenderness ratio (kl/r) over 8. For example, the decrease of the ultimate capacity of the Specimens 12-S-90, 16-S-120 and 20-S-150 (with a slenderness ratio changed from 12 to 20) compared to Specimens 8-S-60, which was, 12%, 27% and 32%, respectively. This highlighted the fact that the recommended slenderness ratio for design purposes of CFFT columns should be reduced to 12. On the other hand, changing the type of internal longitudinal reinforcements from steel to CFRP bars did not significantly affect the ultimate capacity of any two identical specimens (have the same height and FRP tube type). The results indicated that the CFRP-reinforced CFFT columns (8-C-60, 12-C-90, 16-C-120 and 20-C-150) resulted in 13%, 7%, 5% and 0% reductions, respectively, in concentric column capacity as compared to the counterparts steel-reinforced CFFT columns.
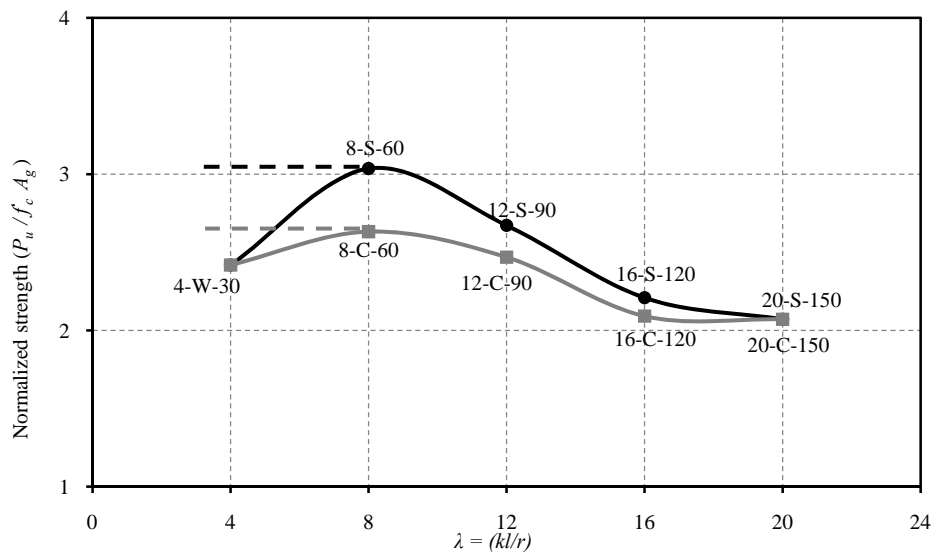
Figure 3. Normalized strength versus slenderness ratio of steel and CFRP-reinforced CFFT columns

3.2   Modes of Failure

The slenderness ratio of the steel and CFRP-reinforced CFFT columns is the main parameter affecting the modes of failure in this study. The FRP tube rupture and/or column instability were the dominant failure mode for the CFFT specimens depending on the slenderness ratio. The unreinforced CFFT specimens (l = 305 mm-Group No. 1) failed in compression due to the rupture of the FRP tube at ultimate resulting from the dilation of the concrete. Figure 4 shows the different failure modes for steel and CFRP-reinforced CFFT columns, respectively. For the columns with a slenderness ratio 8 and 12 (l=610 mm and l= 912 mm), the failure modes were a combination of rupture of the confining FRP tubes and local buckling of internal reinforcing bars at the column mid-height. Yet the CFFT columns have not failed due to instability and the column response was similar to that of short columns. However, the columns with slenderness

First Middle East Conference on Smart Monitoring,
Assessment and Rehabilitation of Civil Structures
8 – 10 February 2011, Dubai, UAE

SMAR 2011

ratio 12 started to buckle at load level that was slightly less than the failure load of the column. Increasing the slenderness ratio to 16 (l=1216 and longer) changed the modes of failure to instability of the CFFT columns. The columns of slenderness ratio 16 and 20 failed at a load level that was much less than the ultimate capacity of the corresponding cylinder (Group No. 1). The instability was evident in the shape of a single curvature mode at a load level around 85% of the final failure load of each specimen. This indicated that these specimens behaved as long columns. Although the column started to buckle at a load level of 85% of the failure load, the deflected column was still stable and carried more axial load. Loading the specimens continued until the specimens could not maintain the applied axial force or until reaching the maximum displacement capacity of the testing machine. The recorded failure modes of the CFFT columns tested with slenderness ratio 16 and 20 showed that the greater the slenderness ratio, the more significant the curvature of the specimen.

Crack patterns of the concrete core were examined by removing the FRP tube after failure. Figure 4.c shows the failure modes of the concrete cores for the different CFRP-reinforced CFFT columns. Limited vertical cracks were observed distributed around the hoop direction of the specimens. For the columns with a slenderness ratio 8 and 12 (l=608 mm and l= 912 mm), concrete compression crushing and CFRP bars rupture were observed at the quarter-length. This is attributed to the fact that the rupture of the FRP tubes started at this zone. On the other hand, the columns with a slenderness ratio 16 and 20 (l=1216 mm and l= 1520 mm) broke right at mid-length, as might be expected from buckling phenomenon. The columns underwent asymmetric breaks-about half of them. Also, concrete compression fracture and CFRP bars rupture were observed at compression side at this zone, while excessive asymmetric flexural cracks were developed at the other side (tension side). The larger bending moment at the mid-length of course was attributed to the start of the fracture at mid-length and the complete failure of the columns.

a. Steel-reinforced CFFT columns   b. CFRP-reinforced CFFT columns   c. Concrete core of CFRP-CFFT
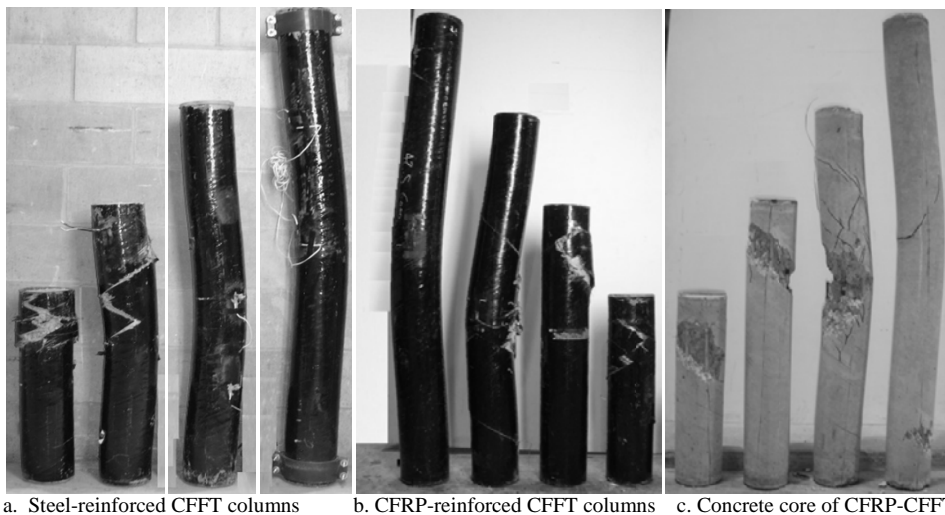
Figure 4. Failure modes of steel and CFRP-reinforced CFFT columns

3.3   Buckling Behavior of Steel and CFRP-CFFT

The post buckling behavior of CFFT columns is shown in Figures 5.a and b in terms of the load-lateral displacement relationships. In each figure, the test results were presented for the counterparts specimens, steel and CFRP-reinforced CFFT columns. For short columns of slenderness ratio 8 and 12, no lateral deformation was recorded due to axial loading. However

First Middle East Conference on Smart Monitoring,
Assessment and Rehabilitation of Civil Structures
8 – 10 February 2011, Dubai, UAE

SMAR 2011
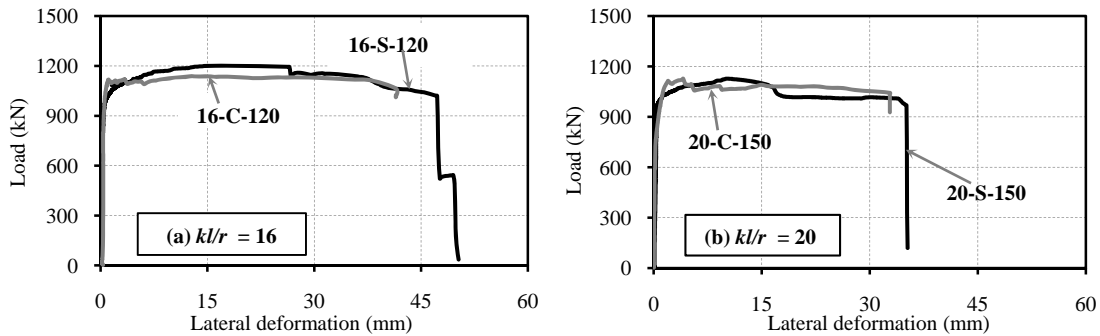
Figure 5. Load verses lateral deformation relationships for steel and CFRP-reinforced CFFT columns

with a higher slenderness ratio; the lateral displacement of the columns was significant indicating instability of the columns. The CFFT columns with a slenderness ratio larger than 12 started to exhibit lateral deformation tendency after load levels around 80% of the failure load. After this load level, the lateral displacement increased rapidly with a significant decrease in the ultimate capacity up to the complete instability of the column. These columns were buckled in a single curvature with a sign-function shape. Figure 5 shows that the counterparts, steel and CFRP-reinforced CFFT columns underwent similar lateral deformations approximately at the same load level. It can be concluded that the flexural capacities are similar for the two counterparts, steel and CFRP-reinforced CFFT columns.

4   CONCLUSION

Based on the specific findings of this research, the following conclusions may be drawn:

1- The experimental investigation conducted in this study indicated that the CFRP bars could be used as a longitudinal reinforcement for CFFT columns, as it behaved similar to that reinforced with steel bars.
2- The test results indicated that the axial capacity of CFRP-reinforced CFFT resulted in 13%, 7%, 5% and 0% reduction as compared to steel-reinforced CFFT columns that had slenderness ratios 8, 12, 16 and 20, respectively.
3- The axial compressive strength of steel and CFRP-reinforced CFFTs was reduced by 13% to 32% with increasing the slenderness ratio from 4 to 20.
4- The test results indicated that the recommended slenderness ratio for design purposes of steel and CFRP-reinforced CFFT columns should be reduced to 12.

5   AKNOWLEDGEMENTS

6   REFERENCES

Al-Sayed, S.H., Al-Salloum, Y.A., and Almusallam, T.H., 2000. Performance of glass fiber reinforced plastic bars as a reinforcing material for concrete structures. *Journal Composites Part B: Engineering*, Vol. 31, Issues 6-7, 555-567.
ASTM. 2008a. Standard test method for apparent hoop tensile strength of plastic or reinforced plastic pipe by split disk method. D 2290-08, West Conshohocken, Pa.
ASTM. 2008b. Standard test method for tensile properties of plastics. D638-08, West Conshohocken, Pa.

First Middle East Conference on Smart Monitoring,
Assessment and Rehabilitation of Civil Structures
8 – 10 February 2011, Dubai, UAE

SMAR 2011

ASTM. 2009. Standard specification for deformed and plain carbon steel bars for concrete reinforcement. A615/A615M-09, West Conshohocken, Pa.

Choo, C, C., Harik, E, I., and Gesund, H. 2006. Strength of rectangular concrete columns reinforced with fiber-reinforced polymer bars. *ACI Structural Journal*, V. 103, 3: 452-459.

Fam, A., Green, R., and Rizkalla, S. 2003. Field application of concrete-filled FRP tubes for marine piles. *ACI Special Publication*, SP-215-9, 161-180.

Kobayashi, K., Fujisaki, T. (1995), "Compressive behaviour of FRP reinforcement in non-prestressed concrete members", in Taerwe, L. (Eds), *Non-metallic Reinforcement for Concrete Structures*, E. & F Spon, London, pp.267-74.

Masmoudi, R., Thériault, M., and Benmokrane, B. "Flexural behaviour of concrete beams reinforced with deformed fibre reinforced plastic reinforcing rods," *ACI Structural Journal*, 1998, V. 95: 6, 665-76.

Mirmiran, A., Shahawy, M., and Beitleman, T. 2001. Slenderness limit for hybrid FRP concrete columns. *Journal of Composites for Construction*, ASCE, Vol. 5, No.1, pp. 26-34.

Mohamed, H., and Masmoudi, R. 2010. Axial load capacity of reinforced concrete-filled FRP tubes columns: experimental versus theoretical predictions. *Journal of Composites for Construction*, ASCE, Vol. 14, 2: 231-243.

Mohamed, H., and Masmoudi, R. 2008. Compressive behaviour of reinforced concrete filled FRP tube. *ACI Special Publications* (SP), SP-257-6, 91-109.

Mohamed, H., Abdel Baky, H., and Masmoudi, R. 2010. Nonlinear stability analysis of concrete filled FRP-tubes columns: experimental and theoretical investigation. *ACI Structural Journal*, Vol. 107, No. 6, pp. 1-10.

Wu, W.P. 1990. Thermo-mechanical properties of fibre reinforced plastic (FRP) bars. West Virginia, University, Morgantown, WV., PhD dissertation.